Utrecht University

Faculty of Geosciences
Physical Geography

Gerben Ruessink
Utrecht University, Netherlands
(b.g.ruessink@uu.nl)
www.uu.nl/staff/bgruessink

EGU2023-3510

Observations of aeolian activity on the deflation floor of a foredune trough blowout

1. Introduction

Background

Blowouts in coastal foredunes provide efficient pathways for wind-driven sand transport inland. In this way, blowouts affect beach-dune sand budgets and facilitate landward dune migration under sea-level rise.

Problem definition

We have limited empirical data and understanding of the short-term (hours) aeolian activity in blowouts and how this activity builds up to longer term blowout dynamics. Data in Hesp and Pringle (2001) indicate that, in contrast to common belief, aeolian activity may not be limited to winds blowing parallel to the blowout axis but can occur for virtually all winds with an onshore component (180° wide arc).

Aim

To study the dependence of aeolian activity in a trough blowout on offshore wind speed and direction for a wide range of conditions.

2. Methodology

Field site

The study site is a trough blowout (Fig. 1a) in the foredune of Dutch National Park Zuid-Kennemerland (Ruessink et al., 2018). The blowout is rectangular in shape, with an ≈100-m long and 25-m wide deflation floor and steep, ≈10-m high lateral walls (Fig. 1b). The main blowout axis is 280 °N.

Field data

The data used here was collected between October 10, 2022 and March 31, 2023 and consists of (i) photographs of the deflation floor taken by a time-lapse trap camera every one to two hours during the day, (ii) 10-min. average wind speeds and directions (at 1-m height) measured by 4 ultrasonic anemometers (SA1 to SA4 in Fig. 1b), and (iii) 10-min. wind speeds and directions (at 10-m height) from a nearby offshore meteorological station.

Conditions

During the 5.5-month study period offshore wind speeds ranged between 0.2 and 21.5 m/s. Winds approached the study site mostly from southern and southwesterly directions, and were thus highly oblique to the blowout axis. The largest wind speed in the blowout mouth (SA1) was 13.8 m/s.

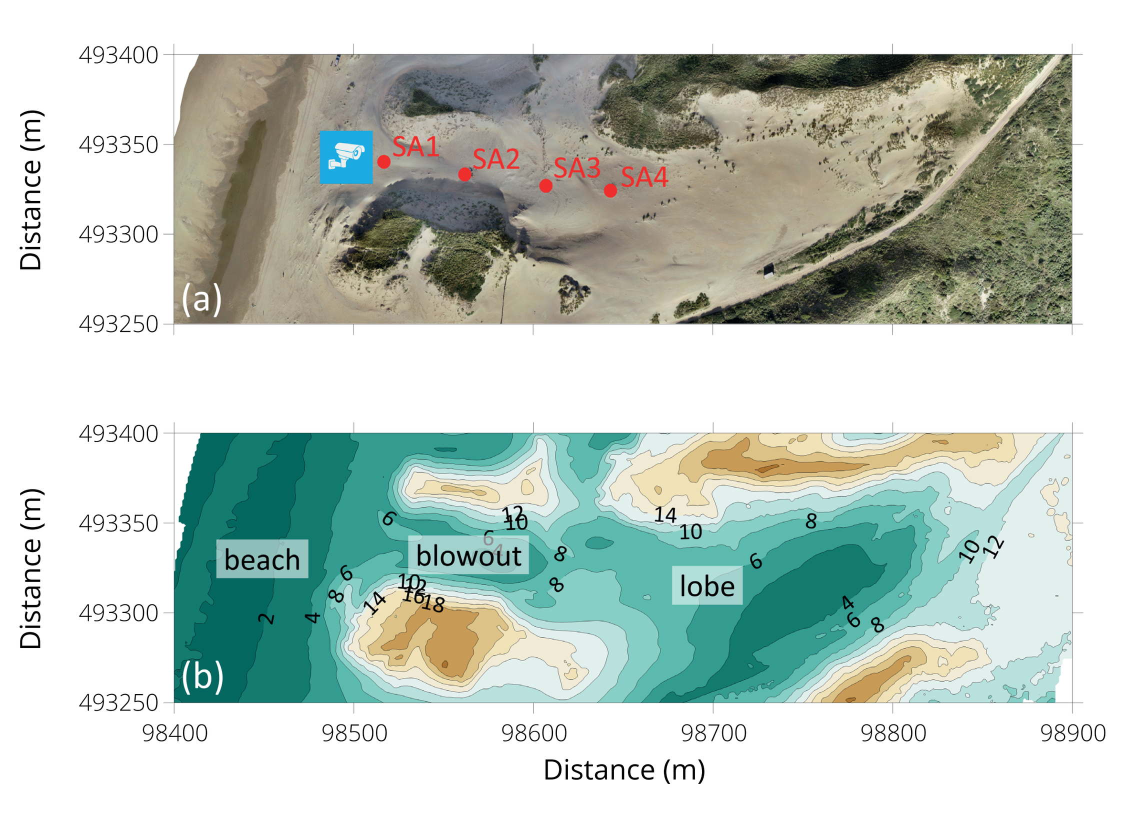

Figure 1

Drone-based (a) orthomosaic and (b) digital elevation model of the study site, collected mid-October 2022. The time-lapse camera is located at the blowout mouth. The four ultrasonic anemometers (SA1 to SA4) are located from the camera (SA1) to the landward end of the blowout (SA3) and on to the depositional lobe (SA4).

Movie on study site:

3. Image classification

Based on Delgado-Fernandez and Davidson-Arnott (2011) and Hage et al. (2018), the aeolian activity in all good-quality images was manually classified in: (0) no activity, (1) traces, and (2) transport (Table 1). Classes (1) and (2) were subdivided in two subclasses based on the intensity of the aeolian activity. In total, 1.237 images were classified: (0) 733, (1) 226, of which 116 in 1a and 100 in 1b, and (2) 278, of which 158 in 2a and 120 in 2b.

Table 1 Image classification scheme

Class	Subclass	Activity	Description
0		None	No aeolian activity, also not in a sequence of images
1	a	Minor traces	Change in image sequence limited to small part of the deflation floor
	b	Moderate traces	Change in image sequence on most of the deflation floor; migration of sand patches; no streamers (Fig. 2a).
2	a	Medium transport	A few individual streamers, sometimes together with unstructured sand patches (Fig. 2b)
	b	Strong transport	Streamers on the entire deflation floor, often together with slipface-less, large-scale bedforms (Fig. 2c)

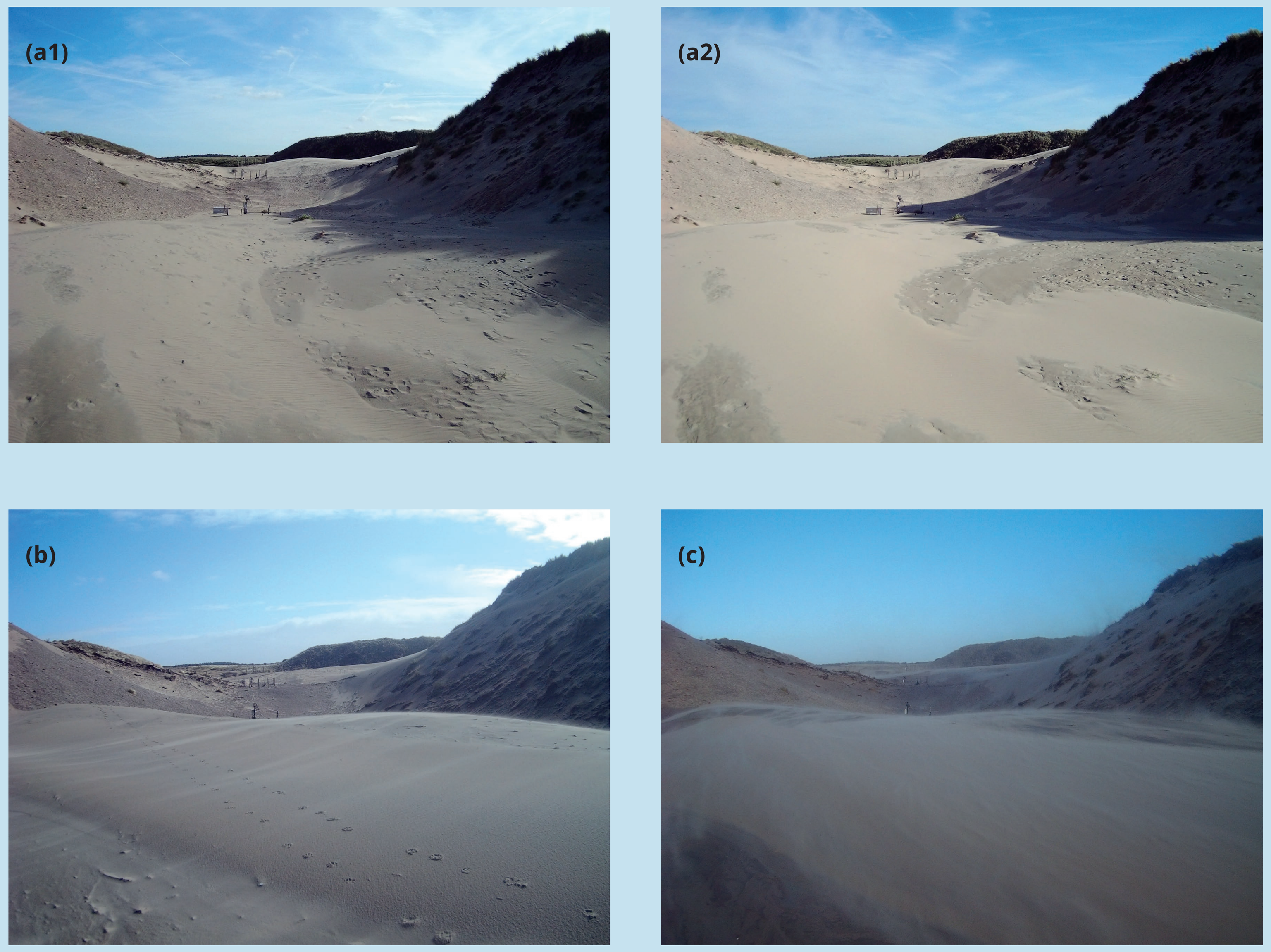

Figure 2

Example images with (a1-2) moderate traces of aeolian activity – class 1b, (b) medium transport – class 2a and (c) strong transport – class 2b. The images in (a1) and (a2) were taken two hours apart. The offshore wind conditions were: (a1-a2) ≈8 m/s, 95 °N, (b) 12.4 m/s, 345 °N and (c) 18.9 m/s, 224 °N. The instruments that can be seen in the blowout are SA2, SA3 and SA4.

References

- Delgado-Fernandez, I. and Davidson-Arnott, R., 2011. Meso-scale aeolian sediment input to coastal dunes: the nature of aeolian transport events. *Geomorphology*, 126, 217-232.
- Hage, P., Ruessink, G. and Donker, J., 2018. Using Argus video monitoring to determine limiting factors of aeolian sand transport on a narrow beach. *Journal of Marine Science and Engineering*, 6, 138; doi:10.3390/jmse6040138.
- Hesp, P.A. and Pringle, A., 2001. Wind flow and topographic steering within a trough blowout. *Journal of Coastal Research*, Special Issue 34, 597-601.
- Ruessink, B.G., Arens, S.M., Kuipers, M. and Donker, J.J.A., 2018. Coastal dune dynamics in response to excavated foredune notches. *Aeolian Research*, 31, 3-17.

4. Main findings

- The classes (1 – traces) and (2 – transport) are observed for a wide range of wind approach angles (± 90° of blowout axis), Fig. 3a. For all these directions the wind is steered into the blowout.
- Classes 1 and 2 have offshore wind speeds exceeding ≈ 5 and 9 m/s, respectively, Fig. 3a.
- Strong transport (2b) is found for offshore wind approach angles up to 70° from the blowout axis with offshore wind speeds > 10 m/s, Fig. 3a. During these conditions the wind speed increases over the deflation floor in the landward direction: the ratio of wind speed at SA3 and SA1 exceeds 1, Fig. 3b.
- For larger approach angles from the blowout axis, the wind increasingly bypasses the blowout (Fig. 3c). The ratio of wind speed at SA1 and the offshore station drops to about 0.2 for ≈70 – 90° from the blowout axis. Accordingly, strong transport is no longer seen for such oblique winds, even though the offshore wind speed may still exceed 10 m/s.

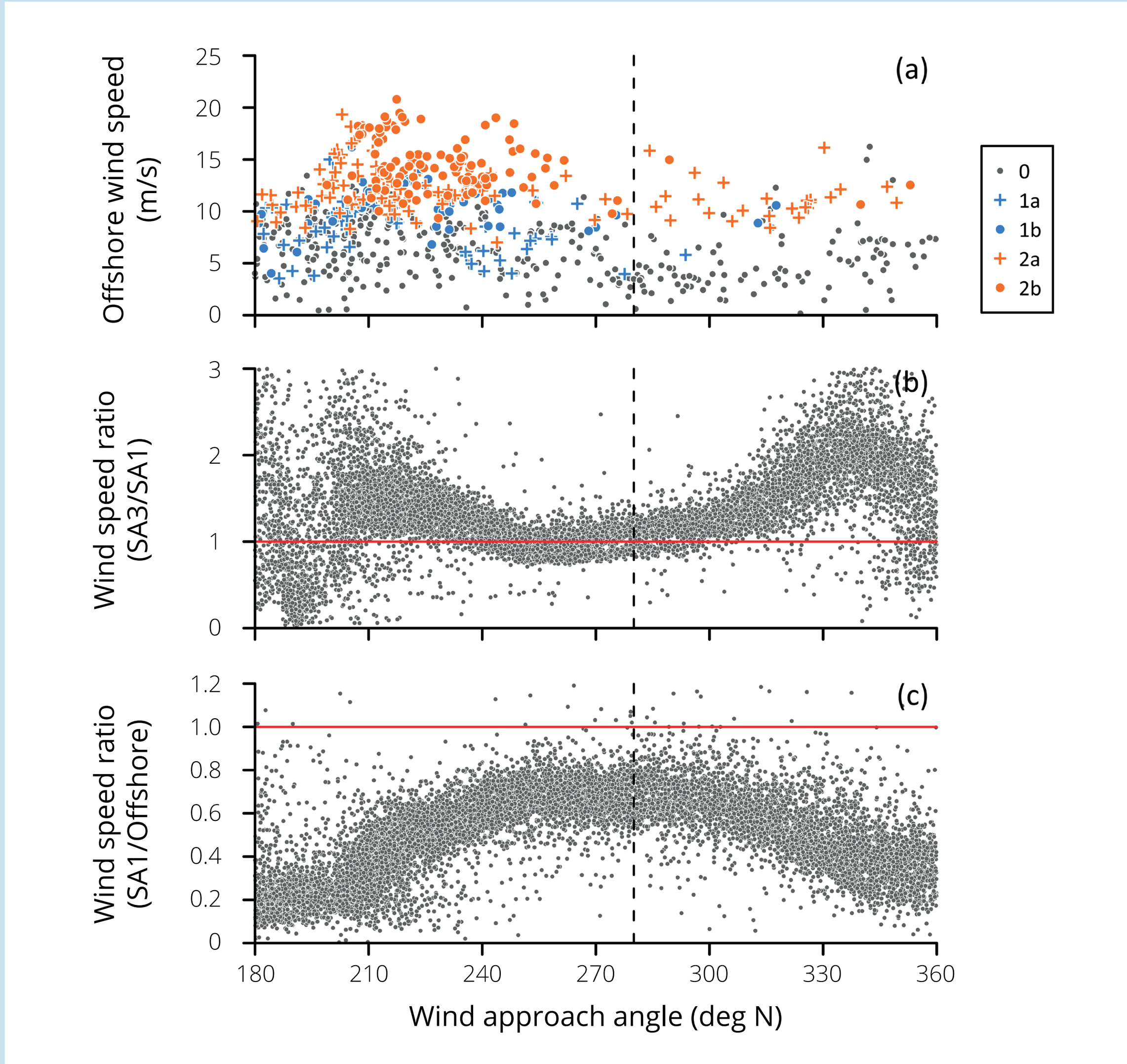

Figure 3

(a) Offshore wind speed of classified images, (b) ratio of wind speed in the blowout SA3/SA1, and (c) ratio of wind speed in blowout and offshore versus the offshore wind approach angle. The vertical dashed line in all panels is the blowout axis (280°N) and the red line in (b) and (c) represents a ratio of 1. Panels (b) and (c) show all available data.

5. Conclusions

- Virtually any, sufficiently strong wind with an onshore component (± 90° from blowout axis) can induce aeolian activity on the deflation floor.
- The intensity of aeolian activity lessens for the most oblique angles (>70° from blowout axis) because the wind increasingly bypasses the blowout.

In agreement with Hesp and Pringle (2001), the main implication of the present work is that the long-term evolution of blowout morphology may not be primarily governed by winds blowing parallel to the blowout axis but by winds from a wide range of approach angles.